MNRAS **000**, 1–11 (2020) Preprint 25 August 2020 Compiled using MNRAS LATEX style file v3.0

Eccentric Dynamical Tides

Yubo Su[1], Dong Lai[1]

[1] *Cornell Center for Astrophysics and Planetary Science, Department of Astronomy, Cornell University, Ithaca, NY 14853, USA*

Accepted XXX. Received YYY; in original form ZZZ

ABSTRACT

Abstract

Key words: keywords

1 INTRODUCTION

Many massive stars are in binaries. Likely progenitors of BNS, HMXRB. Open question: after first SN, does the binary circularize before second SN? Dynamical tides in the radiative envelope are likely to be important, but are hard to calculate in eccentric binaries.

The dissipation due to the dynamical tide in a massive star's envelope under the influence of a *circular* perturber is well understood (Kushnir et al. 2017).

It is also well known that the perturbing potential of an eccentric companion can be decomposed into Fourier harmonics (e.g. Storch & Lai 2013; Vick et al. 2017).

In this paper, we show that the dynamical tide due to an eccentric companion can be approximated in closed form for a wide range of physical parameters. In Section 2, we review the relevant equations. In Section 3, we present novel approximations for the Hansen coefficients. In Section 4, we apply these approximations to obtain closed forms for the torque and energy transfer rate in the binary. In Section 5, we apply our theory to observations. In Section 6, we discuss and conclude.

2 SUMMARY OF EXISTING WORK

2.1 Decomposition of Perturbation from an Eccentric Companion

Consider a star subject to the perturbing potential of a companion star with mass M_2, For a general eccentric orbit, the potential to quadrupolar order can be decomposed into a sum over circular

orbits (Storch & Lai 2013; Vick et al. 2017):

$$U = \sum_m U_{2m}(\vec{r}, t), \tag{1}$$

$$\begin{aligned} U_{2m}(\vec{r}) &= -\frac{GM_2 W_{2m} r^2}{D(t)^3} e^{-imf(t)} Y_{2m}(\theta, \phi), \\ &= -\frac{GM_2 W_{2m} r^2}{a^3} Y_{2m}(\theta, \phi) \sum_{N=-\infty}^{\infty} F_{Nm} e^{-iN\Omega t}, \end{aligned} \tag{2}$$

$$F_{Nm} = \frac{1}{\pi} \int_0^{\pi} \frac{\cos\left[N(E - e\sin E) - mf(E)\right]}{(1 - e\cos E)^2} \, \mathrm{d}E. \tag{3}$$

We denote $W_{2\pm2} = \sqrt{3\pi/10}$, $W_{2\pm1} = 0$, $W_{20} = -\sqrt{\pi/5}$, $D(t)$ the instantaneous distance between the star and companion, $f(t)$ the true anomaly, Y_{lm} the spherical harmonics, and Ω the mean motion of the companion. Note that F_{Nm} are the *Hansen coefficients* for $l = 2$. The total torque on the star, energy transfer in the inertial frame, and heating in the star's corotating frame are given respectively (Vick et al. 2017):

$$\tau = \sum_{N=-\infty}^{\infty} F_{N2}^2 \hat{\tau}(\omega = N\Omega - 2\Omega_s), \tag{4}$$

$$\dot{E}_{\rm in} = \frac{1}{2} \sum_{N=-\infty}^{\infty} \left[\left(\frac{W_{20}}{W_{22}} \right)^2 N\Omega F_{N0}^2 \hat{\tau}(\omega = N\Omega) + N\Omega F_{N2}^2 \hat{\tau}(\omega = N\Omega - 2\Omega_s) \right], \tag{5}$$

$$\dot{E}_{\rm rot} = \dot{E}_{\rm in} - \Omega_s \tau, \tag{6}$$

where $\hat{\tau}(\omega)$ is the torque exerted by a perturber on a circular trajectory with orbital frequency ω. Compared to Vick et al. (2017), we use $\tau_N(\omega) = T_0 \, \mathrm{sgn}(\omega) \hat{F}(|\omega|)$, for better integration with the next section.

2.2 Tidal Torque in Massive Stars

For a circular orbit with orbital frequency ω and fixed semimajor axis a, the tidal torque exerted on the star by the companion is given by Kushnir et al. 2017:

$$\tau(\omega) = \hat{\tau}(r_c, \omega) \, \mathrm{sgn}\left(1 - \frac{2\Omega_s}{\omega}\right) \left| 1 - \frac{2\Omega_s}{\omega} \right|^{8/3}, \tag{7}$$

$$\begin{aligned} \hat{\tau}(r_c, \omega) &= \frac{GM_2^2 r_c^5}{a^6} \left(\frac{\omega}{\sqrt{GM_c/r_c^3}} \right)^{8/3} \left[\frac{r_c}{g_c} \left(\frac{\mathrm{d}N^2}{\mathrm{d}\ln r} \right)_{r=r_c} \right]^{-1/3} \frac{\rho_c}{\bar{\rho}_c} \left(1 - \frac{\rho_c}{\bar{\rho}_c} \right)^2 \left[\frac{3}{2} \frac{3^{2/3}\Gamma^2(1/3)}{5 \cdot 6^{4/3}} \frac{3}{4\pi} \alpha^2 \right], \\ &\equiv \beta_2 \frac{GM_2^2 r_c^5}{a^6} \left(\frac{\omega}{\sqrt{GM_c/r_c^3}} \right)^{8/3} \frac{\rho_c}{\bar{\rho}_c} \left(1 - \frac{\rho_c}{\bar{\rho}_c} \right)^2. \end{aligned} \tag{8}$$

Here, $1 - \frac{2\Omega_s}{\omega}$ is the dimensionless pattern frequency, α is defined in Equation A32 of Kushnir et al. 2017, r_c is the radius of the core, M_c the mass of the core, g_c is the gravitational acceleration at the

radiative-convective boundary (RCB), N^2 is the Brunt-Vaisala frequency, r is the radial coordinate within the star, ρ_c is the density at the RCB, $\bar{\rho}_c$ is the average density of the convective core, and $\beta_2 \approx 1$ is a good approximation for a large range of stellar models (Kushnir et al. 2017).

2.3 Objective of This Paper

Putting the two results from the previous two sections together, we can immediately obtain the tidal torque due to an eccentric companion:

$$\tau = \sum_{N=-\infty}^{N=\infty} F_{N2}^2 \tau_N, \tag{9}$$

where

$$\tau_N(r_c) = \hat{\tau}(r_c)\mathrm{sgn}\left(N - \frac{2\Omega_s}{\Omega}\right)\left|N - \frac{2\Omega_s}{\Omega}\right|^{8/3}, \tag{10}$$

and the corresponding energy transfer rate

$$\dot{E}_{\rm in} = \frac{\hat{\tau}(r_c,\Omega)}{2}\sum_{N=-\infty}^{\infty}\left[N\Omega F_{N2}^2 \mathrm{sgn}\left(N - 2\Omega_s/\Omega\right)|N - 2\Omega_s/\Omega|^{8/3} + \left(\frac{W_{20}}{W_{22}}\right)^2 \Omega F_{N0}^2 |N|^{11/3}\right]. \tag{11}$$

While exact, these expressions are difficult to evaluate for larger eccentricities, where one often must sum hundreds or thousands of terms. In the subsequent sections, we present closed-form approximations to the above equations.

3 APPROXIMATING HANSEN COEFFICIENTS

3.1 $m = 2$ Hansen Coefficient Behavior at High Eccentricity

Recall that the Hansen coefficients are defined as the Fourier series coffecients of part of the disturbing function

$$\frac{a^3}{D(t)^3} e^{-imf} = \sum_{N=-\infty}^{\infty} F_{Nm} e^{-iN\Omega t}. \tag{12}$$

Observe that $F_{(-N)m} = F_{N(-m)}$. We further observe the following facts about the Hansen coefficients F_{N2}:

- For substantial eccentricies, F_{N2} has only one substantial peak. The only characteristic scale for N is $N_{\rm p}$ the pericenter harmonic, so indeed we find the peak of F_{N2} occurs at $\sim N_{\rm p}$ (see Fig. 1). Furthermore, for $N < 0$, $F_{N2} \approx 0$ to good accuracy.
- Since the left hand side of Eq. (12) is smooth in time, the Fourier coefficients must fall off exponentially for sufficiently large N.

- Since there are no characteristic timescales between Ω and $\Omega_{\rm p}$, we anticipate the Hansen coefficients must be scale free between $N = 1$ and $N_{\rm p}$, i.e. a power law.

As such, we make ansatz for the scalings of the Hansen coefficients for $N \geq 0$:

$$F_{N2} \approx C_2 N^p e^{-N/\eta_2}, \tag{13}$$

Eq. (13) has the advantage that $N_{\rm max} = p\eta_2$ immediately. Since we expect the Hansen coefficients to peak at $N \sim \Omega_{\rm p}/\Omega$, where

$$\Omega_{\rm p} \equiv\simeq \Omega \frac{\sqrt{1+e}}{(1-e)^{3/2}}, \tag{14}$$

is the pericenter orbital frequency, we expect $\eta_2 \propto (1-e)^{-3/2}$ as well.

Note that at moderate eccentricities $e \lesssim 0.7$, p is very poorly constrained, since only the harmonics $N \lesssim N_{\rm max}$ contribute to the fit. Thus, we fix $p = 2$ by fitting F_{N2} for large eccentricities ($e \gtrsim 0.9$) and assume it is universal. We found indeed this proves robust to smaller eccentricities[1].

To constrain the remaining two free parameters η_2 and C_2 the normalization, we use the well known Hansen coefficient homements (Hut 1981; Storch & Lai 2013; Vick et al. 2017):

$$\sum_{N=-\infty}^{\infty} F_{N2}^2 = \frac{1+3e^2+3e^4/8}{\left(1-e^2\right)^{9/2}} \equiv \frac{f_5}{\left(1-e^2\right)^{9/2}}, \tag{15}$$

$$\sum_{N=-\infty}^{\infty} F_{N2}^2 N = \frac{2}{\left(1-e^2\right)^6}\left(1+\frac{15e^2}{2}+\frac{45e^4}{8}+\frac{5e^6}{16}\right), \tag{16}$$

$$= \frac{2f_2}{\left(1-e^2\right)^6}. \tag{17}$$

This fixes

$$\eta_2 = \frac{4f_2}{5f_5\left(1-e^2\right)^{3/2}}, \tag{18}$$

$$C_2^2\eta_2^5 = \frac{4f_5}{3\left(1-e^2\right)^{9/2}}. \tag{19}$$

Note that indeed $\eta_2 \propto \left(1-e^2\right)^{-3/2}$. The agreement of this fit of the Hansen coefficients can be seen in Fig. 1.

[1] There is some numerical justification for p being exactly 2. We note the function $(a/D(t))^3\, e^{-imf}$ resembles the second derivative of a Gaussian: as it is sharply peaked at $t = 0$, but goes negative at some small, positive time, and only becomes positive again near $t = P$ the orbital period. A Gaussian with vanishing width (corresponding to $e \to 1$) approximates the Dirac delta, which has a flat frequency spectrum. This implies the second derivative of the Dirac delta has Fourier coefficients with increasing magnitude $\propto N^2$. Thus, as $e \to 1$, we expect the F_{Nm} to also scale like N^2 for $N \ll \Omega_{\rm p}/\Omega$.

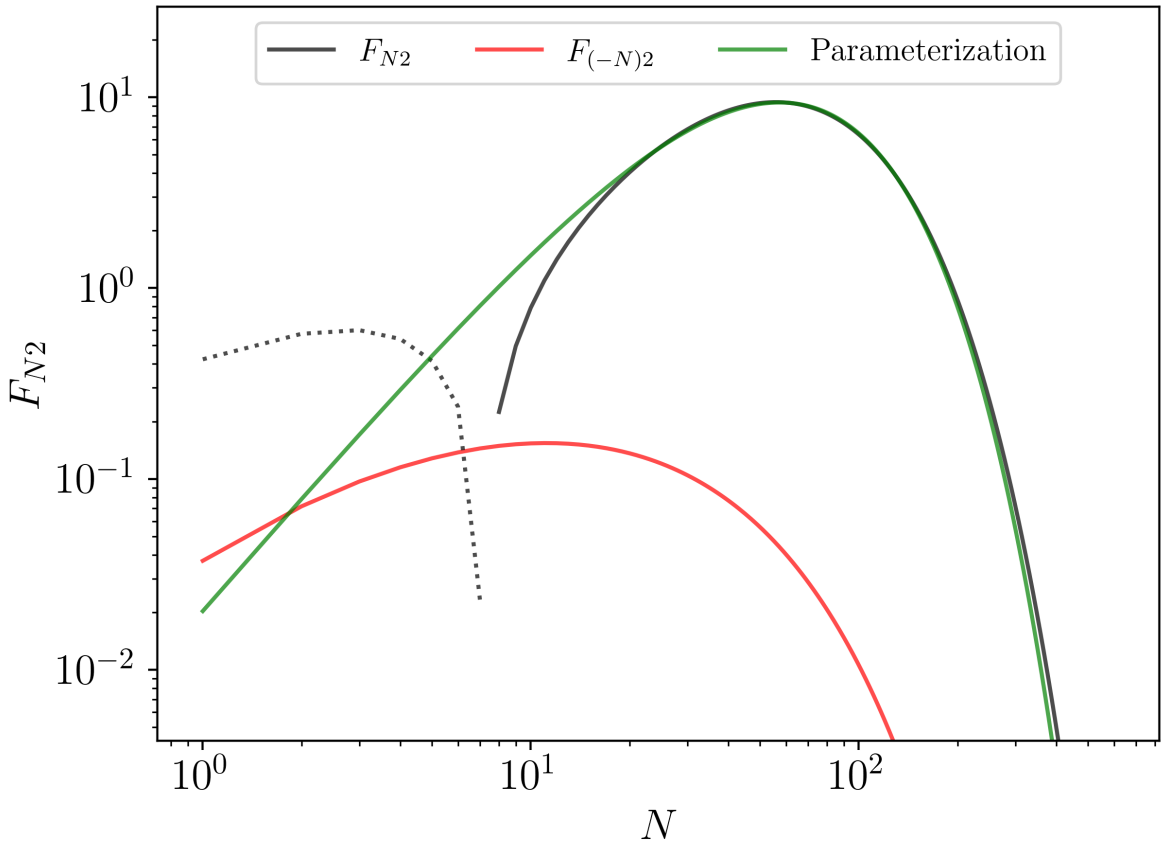

Figure 1. Plot of Hansen coefficients F_{N2}, where dotted lines denote negative values. The green line is the fitted function of form Eq. (13).

3.2 $m = 0$ Hansen Coefficient Behavior at High Eccentricity

These coefficients have only one characteristic scale in harmonic space, namely $\Omega/\Omega_{\rm p}$, but must be symmetric, therefore, the natural ansatz is of form

$$F_{N0} = C_0 e^{-|N|/\eta_0}. \tag{20}$$

Here, again, we expect $\eta_0 \simeq \Omega/\Omega_{\rm p}$. The two free parameters C_0 and η_0 are again fixed by the well known moments (Hut 1981; Storch & Lai 2013; Vick et al. 2017):

$$\sum_{N=-\infty}^{\infty} F_{N0}^2 = \frac{f_5}{\left(1-e^2\right)^{9/2}}, \tag{21}$$

$$\sum_{N=-\infty}^{\infty} F_{N0}^2 N^2 = \frac{9e^2}{2\left(1-e^2\right)^{15/2}} f_3. \tag{22}$$

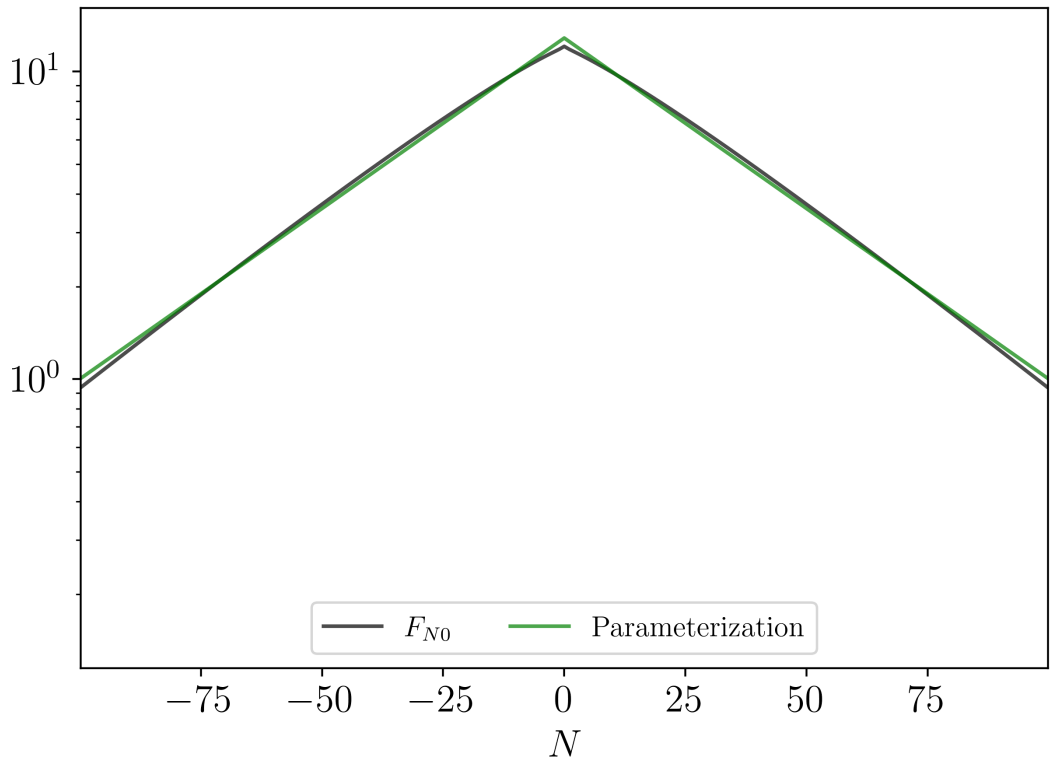

Figure 2. F_{N0} for $e = 0.9$, with fit [Eq. (20)] overlaid.

Integration of the ansatz fixes the two free parameters

$$\eta_0^2 = \frac{9e^2 f_3}{(1-e^2)^3 f_5}, \tag{23}$$

$$C_0^2 \eta_0 = \frac{f_5}{(1-e^2)^{9/2}}. \tag{24}$$

4 EVALUATING TORQUE AND ENERGY TRANSFER

4.1 Tidal Torque

To obtain a closed form for the tidal torque experienced by a massive star due to an eccentric companion, as a first estimate we can use Eq. (7) as the torque generated by each mode in Eq. (4). This gives

$$\tau = \hat{T}(r_c, \Omega) \sum_{N=-\infty}^{\infty} F_{N2}^2 \,\mathrm{sgn}\left(N - 2\frac{\Omega_s}{\Omega}\right) \left|N - 2\frac{\Omega_s}{\Omega}\right|^{8/3}. \tag{25}$$

Using our integral approximations, this immediately becomes

$$\tau = \hat{\tau} \int_0^{\infty} C_2^2 N^4 e^{-2N/\eta_2} \,\mathrm{sgn}\,(N - 2\Omega_s/\Omega)\,|N - 2\Omega_s/\Omega|^{8/3}\ \mathrm{d}N. \tag{26}$$

Note that strictly speaking, this is an upper bound on the tidal torque, as it assumes all excited IGWs damp effectively, but there is evidence this bound may be saturated (see Section 6).

Towards evaluating Eq. (25), we first consider the limit $|\Omega_s| \to \infty$ for simplicity. This requires only the known Hansen coefficient moments, and we obtain

$$\tau = -\hat{\tau}\,\mathrm{sgn}(\Omega_s)\;\; |2\Omega_s/\Omega|^{8/3}\,\frac{f_5}{(1-e^2)^{9/2}}. \tag{27}$$

Next, we consider the case where $N_{\max} \gtrsim 2\Omega_s/\Omega$, where $N_{\max}$ is the N for which the magnitude of the summand in Eq. (25) is largest. We make the ansatz that $N - 2\Omega_s/\Omega$ can be effectively factorized as

$$N - 2\Omega_s/\Omega \simeq \frac{N}{N_{\max}}\left(N_{\max} - \frac{2\alpha\Omega_s}{\Omega}\right), \tag{28}$$

In this case, $N_{\max} = 10\eta_2/3$. α is constrained by requiring our expression reproduce the high spin limit when taking $|\Omega_s| \to \infty$. Then, the torque becomes

$$\tau = \hat{\tau}\frac{f_5\eta_2^{8/3}}{(1-e^2)^{9/2}}\;\mathrm{sgn}\left(1-0.691\frac{\Omega_s}{\eta_2\Omega}\right)\left|1-0.691\frac{\Omega_s}{\eta_2\Omega}\right|^{8/3}\frac{\Gamma(23/3)}{4!}\frac{1}{2^{8/3}}. \tag{29}$$

See Figs. 3, 4, and 5 for the accuracy of this prediction.

4.2 Pseudosynchronization

In fact, Eq. (29) gives a very concrete prediction for the pseudosynchronization frequency:

$$\frac{\Omega_{\mathrm{s,sync}}}{\Omega} = \frac{\eta_2}{0.691}. \tag{30}$$

This has the expected scaling $\Omega_{\mathrm{s,sync}} \propto (1-e^2)^{-3/2}$, but is more accurate than $\Omega_{\mathrm{s,sync}} \simeq \Omega_{\mathrm{p}}$, as seen in Fig. 6.

4.3 Closed Form for Energy Transfer

The integral form is

$$\dot{E}_{\mathrm{in}} = \frac{\hat{\tau}(r_c,\Omega)\Omega}{2}\int_0^\infty\left[C_2^2N^5e^{-2N/\eta_2}\mathrm{sgn}\left(N-2\Omega_s/\Omega\right)|N-2\Omega_s/\Omega|^{8/3} + 2\frac{2}{3}C_0^2e^{-2N/\eta_0}N^{11/3}\right]\mathrm{d}N. \tag{31}$$

This comes out to be (elaborate)

$$\dot{E}_{\mathrm{in}} = \frac{\hat{\tau}\Omega}{2}\Bigg[\mathrm{sgn}\left(1-0.5886\frac{\Omega_s}{\eta_2\Omega}\right)\left|1-0.5886\frac{\Omega_s}{\eta_2\Omega}\right|^{8/3}\frac{f_5}{(1-e^2)^{9/2}}\frac{\Gamma(26/3)}{4!}\left(\frac{\eta_2}{2}\right)^{11/3} + \frac{f_5\Gamma(14/3)}{(1-e^2)^{10}}\left(\frac{3}{2}\right)^{8/3}\left(\frac{e^2f_3}{f_5}\right)^{11/6}\Bigg]. \tag{32}$$

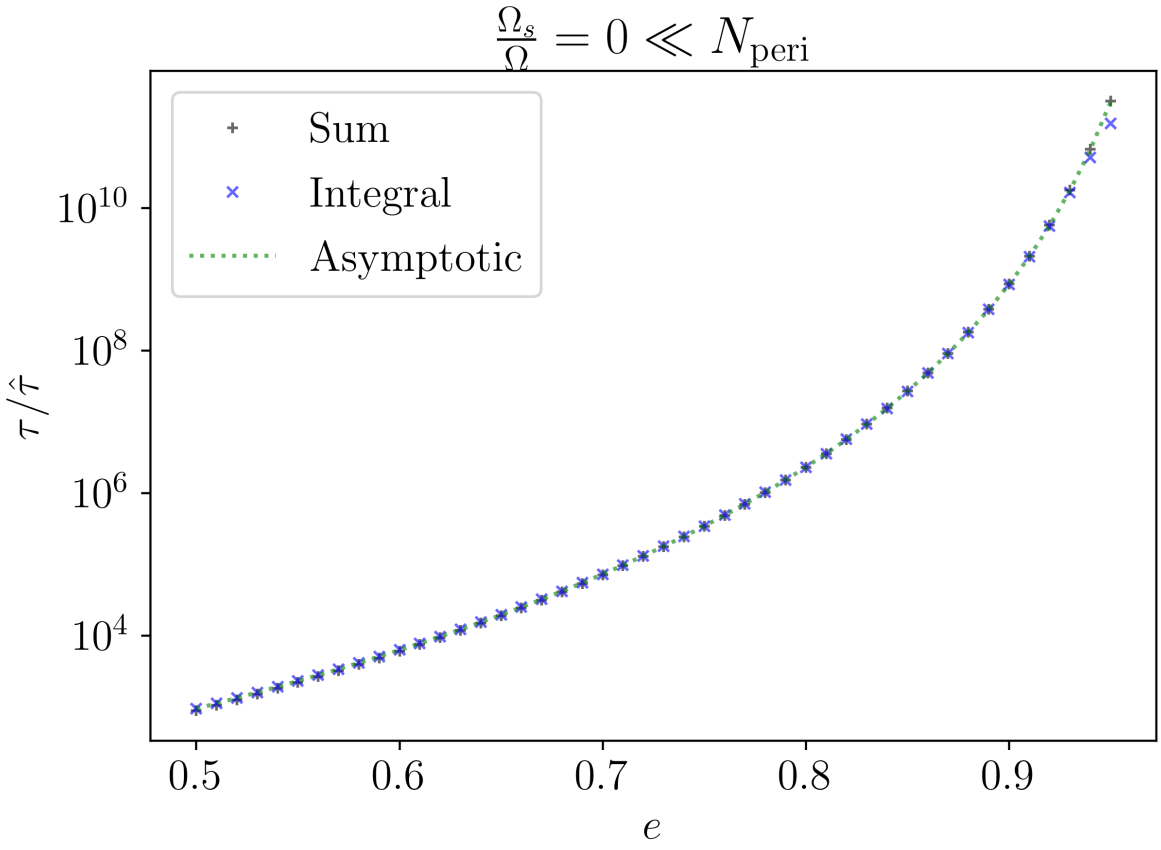

Figure 3. Tidal torque on a non-rotating star with a companion having orbital eccentricity e. Blue plus signs represent explicit summation of Eq. (25), blue crosses are evaluated using the integral approximation Eq. (26), while the green dashed line is Eq. (29).

We make plots in the two Ω_s regimes as a function of eccentricity in Figs. 7 and 8. Agreement is good again.

5 EXAMPLE SYSTEM: J0045+7319

We study J0045+7319 (Bell et al. 1995).

We can arrive at an upper bound for the $\dot{P}$ by setting the spin frequency equal to the breakup frequency. Then, taking the correct parameters and evaluating $\dot{E}_{\rm in}$, we obtain

$$\frac{\dot{P}}{2\pi} \lesssim -\frac{3}{(1+q)^2}\beta_2 \left(\frac{r_c}{a}\right)^5 \frac{\rho_c}{\bar{\rho}_c}\left(1-\frac{\rho_c}{\bar{\rho}_c}\right)^2 2^{8/3}\frac{f_2}{(1-e^2)^6}. \tag{33}$$

This comes out to be $r_c \gtrsim 1.799 R_\odot$ for J0045+7319, larger than the prior values in the literature and much larger than MESA models.

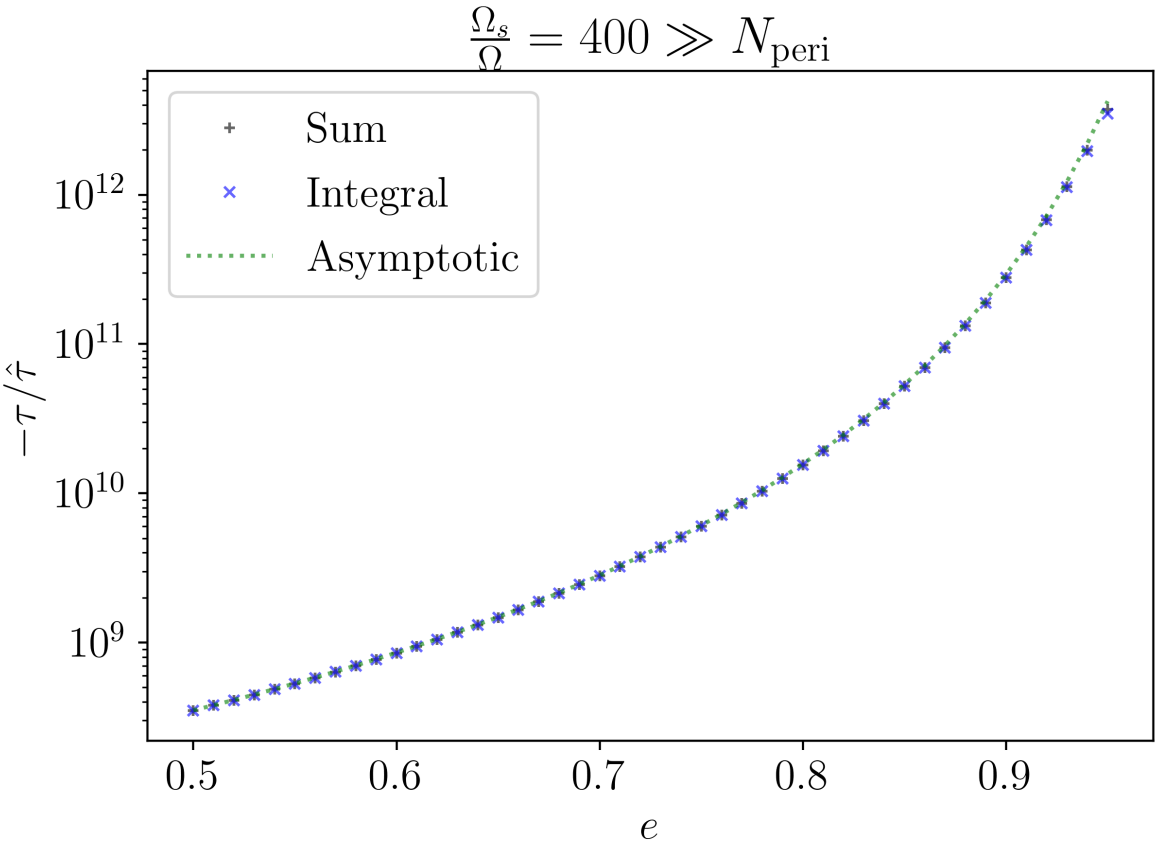

Figure 4. Same as Fig. 3 but for $\Omega_s \gg \Omega_{\rm p}$.

5.1 Stellar Structure Simulations

In previous literature, the primary star was initially taken to have $M_1 = 8.8 M_\odot$ (Kumar & Quataert 1998; Lai 1996), by taking $M_2 \simeq 1.4 M_\odot$ characteristic mass for NSs and multiplying by the observed q. A later, but still very old, study proposed $M_1 \approx 10 M_\odot$ by comparison with stellar models. Using MESA to generate updated stellar models (TODO all citations), we compute an updated M_1 estimate, giving detailed stellar structure measurements.

At the level of approximation of this paper, our procedure is as follows: we use a few different values of convective overshooting and mixing, and metallicities, and compute stellar structures for both both non-rotating and highly rotating $\sim 0.95\Omega_{\rm s,c}$ stars. We find that, in general, to match the observed T, L we must let the star evolve to $\sim 80\%$ of the way to complete core hydrogen depletion. We then sample a range of stellar masses, and find the stellar mass that best reproduces the observed T, L.

For all of these systems, $r_c \lesssim R_\odot$, in tension with our bound above.

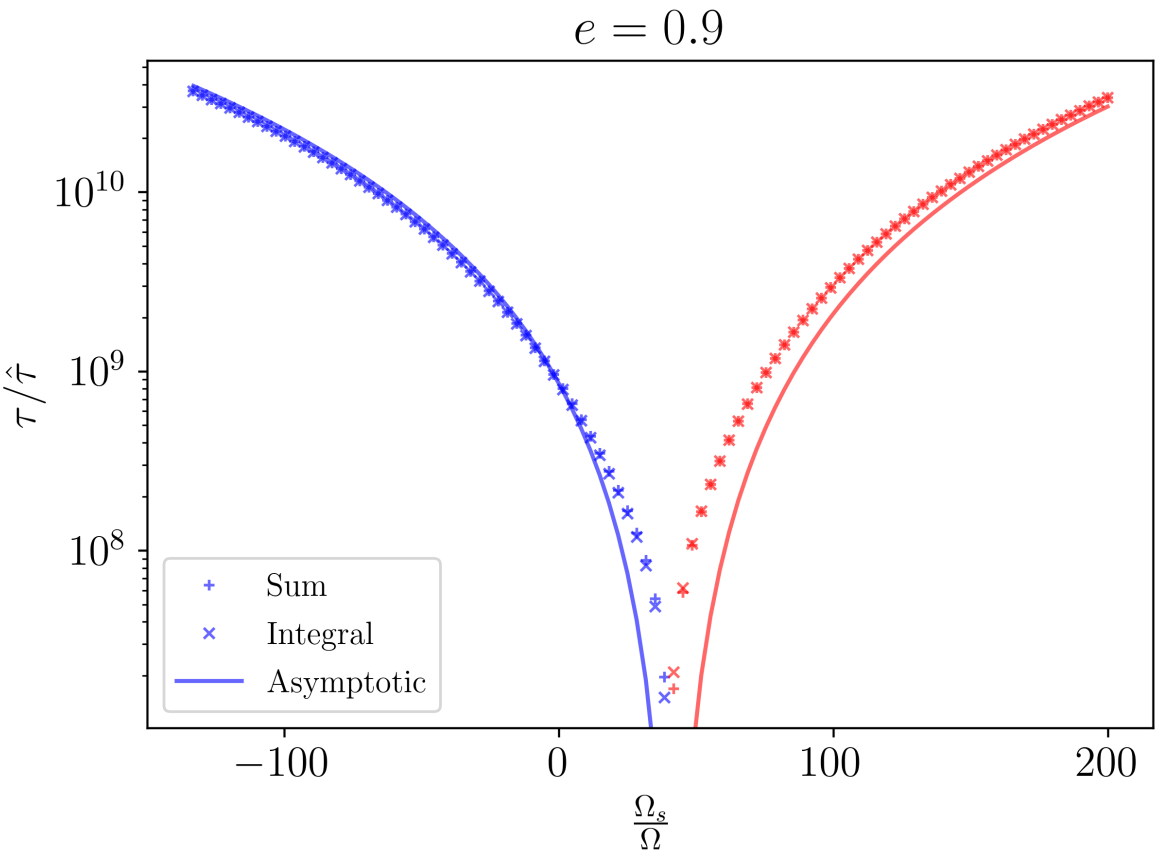

Figure 5. Tidal torque as a function of spin for a highly eccentric $e = 0.9$ companion. Pluses represent direct summation of Hansen coefficients, crosses represent the integral approximation, while solid lines represent the analytic closed form. Blue [red] means positive [negative] torque.

6 CONCLUSION AND DISCUSSION

The primary results of the paper are Eq. (29), shown in Figs. 3, 4, and 5 to be reasonably accurate across a range of spins and eccentricities. The energy dissipation rate is also computed using similar techniques and show good agreement (see Figs. 7 and 8).

- Thanks to some references (Barker & Ogilvie, my work), there seems to be some evidence that hydrodynamic wave breaking could cause all IGW to break and not reflect, once the pericenter wave reaches nonlinear amplitudes.
- As noted in the text, the approximate forms enforce $\mathrm{d}\tau/\mathrm{d}\Omega_s = 0$, which the actual torque does not satisfy. This introduces some slight errors in the exact value of the torque very near pseudosynchronization.

REFERENCES

Bell J., Bessell M., Stappers B., Bailes M., Kaspi V., 1995, The Astrophysical Journal Letters, 447, L117

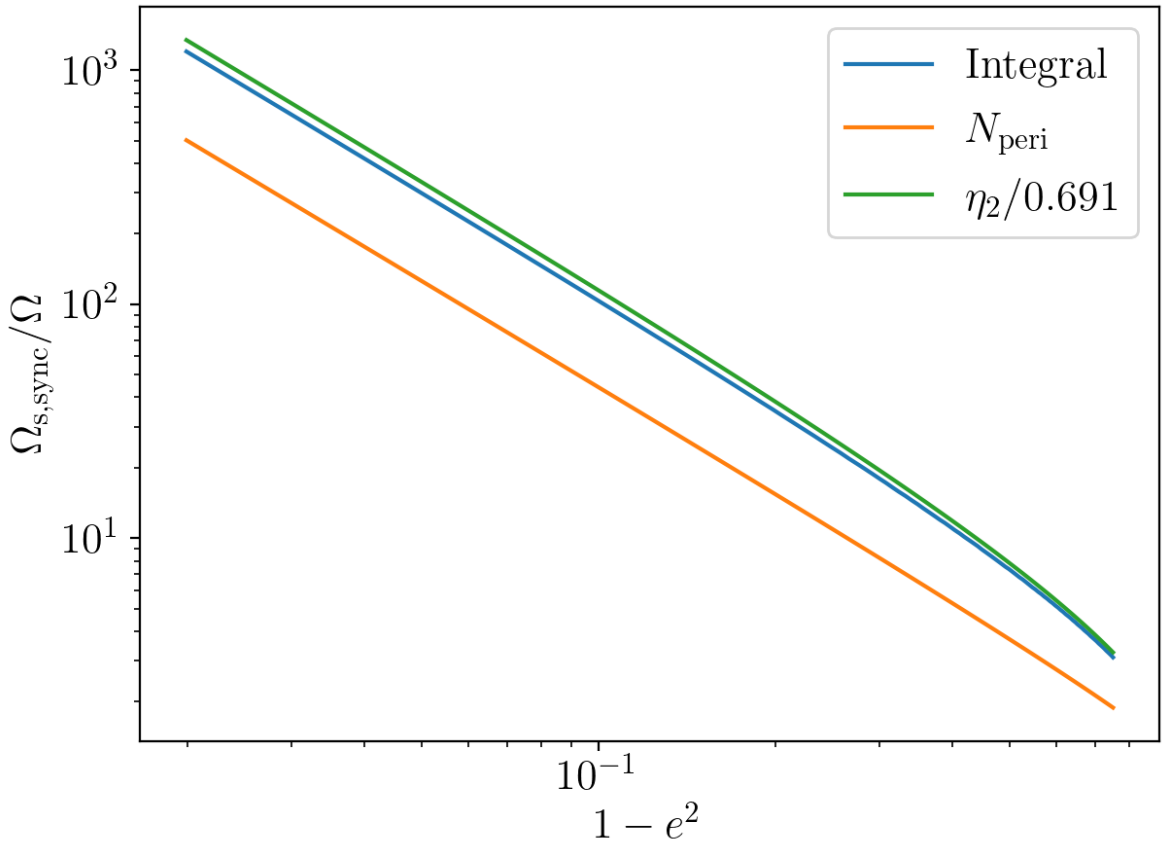

Figure 6. Pseudosynchronization frequency. Integral form is obtained by performing root finding using the integral form for the torque. We see that Eq. (30) is a very good approximation.

Hut P., 1981, Astronomy and Astrophysics, 99, 126

Kumar P., Quataert E. J., 1998, The Astrophysical Journal, 493, 412

Kushnir D., Zaldarriaga M., Kollmeier J. A., Waldman R., 2017, Monthly Notices of the Royal Astronomical Society, 467, 2146

Lai D., 1996, The Astrophysical Journal Letters, 466, L35

Storch N. I., Lai D., 2013, Monthly Notices of the Royal Astronomical Society, 438, 1526

Vick M., Lai D., Fuller J., 2017, Monthly Notices of the Royal Astronomical Society, 468, 2296

This paper has been typeset from a TEX/LATEX file prepared by the author.

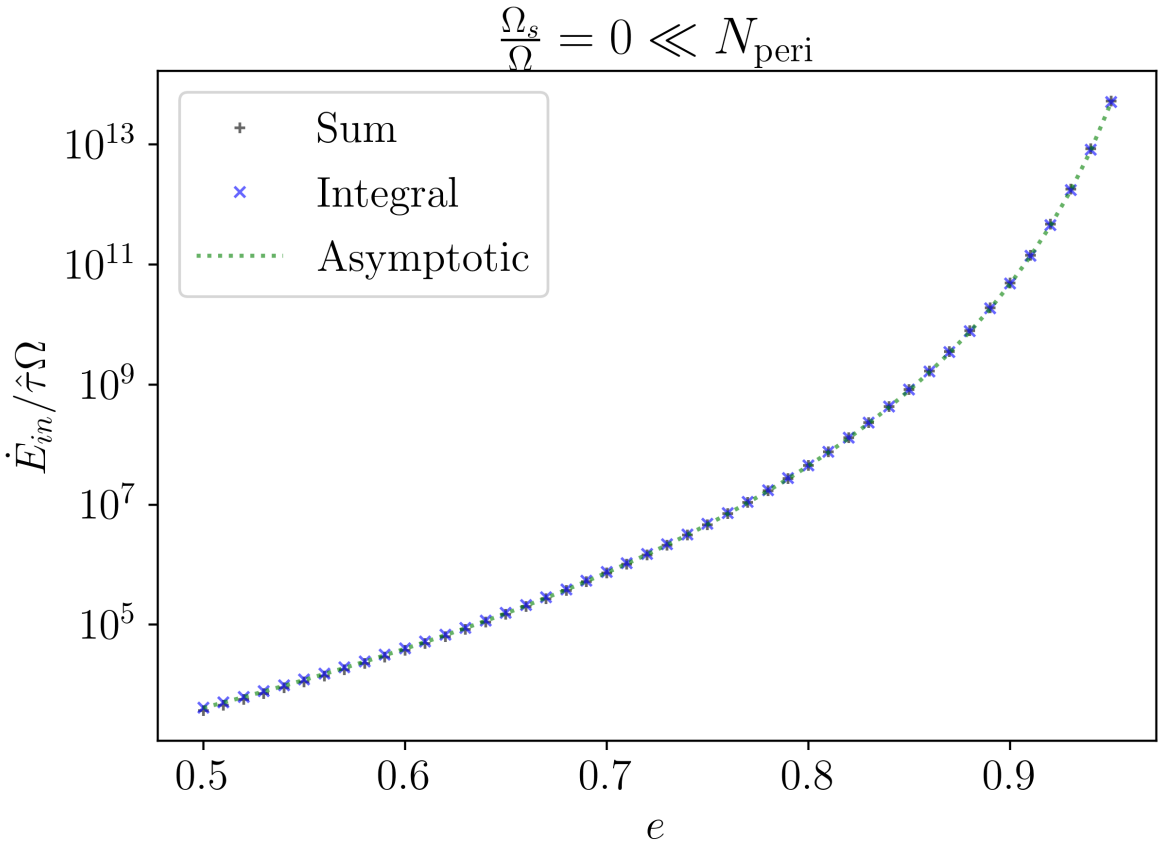

Figure 7. Plot of $\dot{E}_{\rm in}$ for a non-rotating star. Blue pluses represent explicit summation of the Hansen coefficients, crosses the integral form Eq. (31), and the green dashed line the closed form Eq. (32).

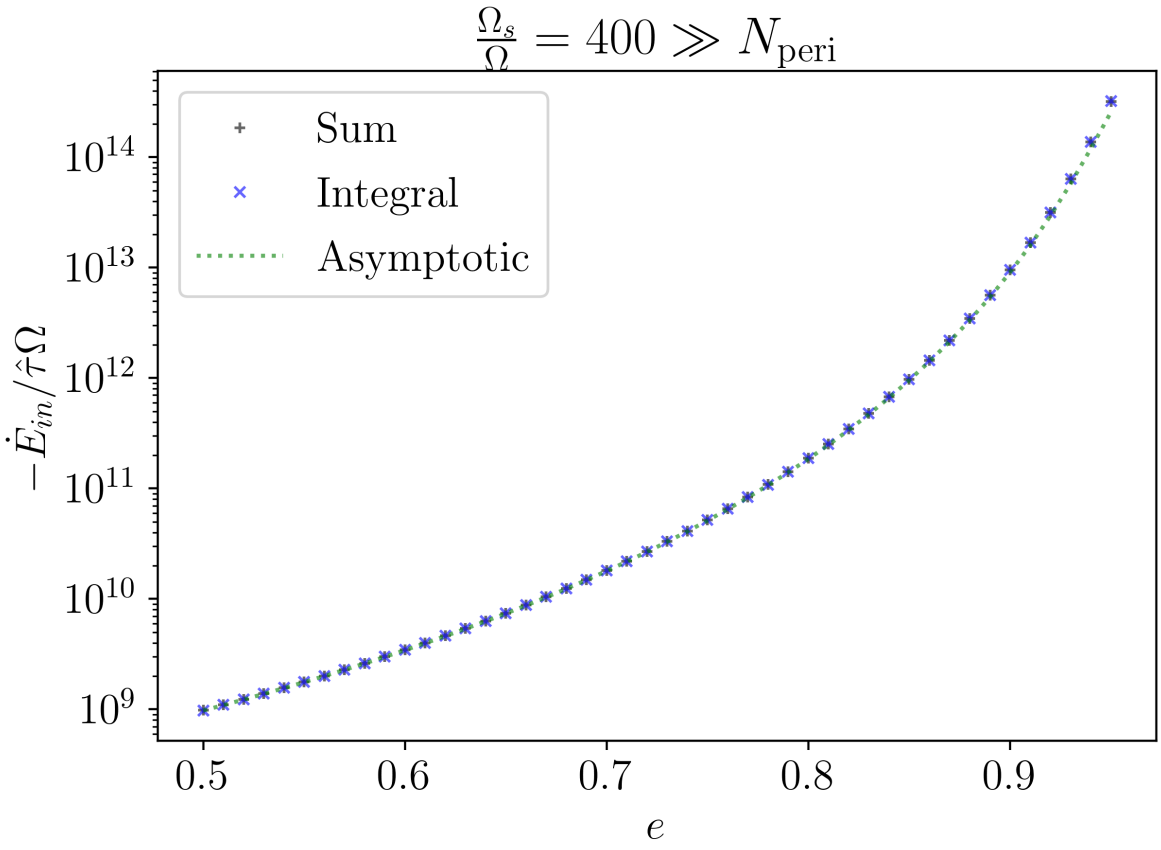

Figure 8. Same as Fig. 7 but for a rapidly spinning star.